Supplementary information

Skin-Integrated Transparent and Stretchable Strain Sensor with Interactive Color-Changing Electrochromic Display

Heun Park,[a] Dong Sik Kim,[a] Soo Yeong Hong,[a] Chulmin Kim,[b] Jun Yeong Yun,[a] Seung Yun Oh,[c] Sang Woo Jin,[c] Yu Ra Jeong,[a] Gyu Tae Kim,[b] and Jeong Sook Ha[a,c*]

[a] Department of Chemical and Biological Engineering, Korea University, 145 Anam-ro, Seongbuk-gu, Seoul, 02841, Republic of Korea

[b] Department of Electrical Engineering, Korea University, 145 Anam-ro, Seongbuk-gu, Seoul, 02841, Republic of Korea

[c] KU-KIST Graduate School of Converging Science and Technology, Korea University, 145 Anam-ro, Seongbuk-gu, Seoul, 02841, Republic of Korea

* Address correspondence to Jeong Sook Ha, jeongsha@korea.ac.kr.

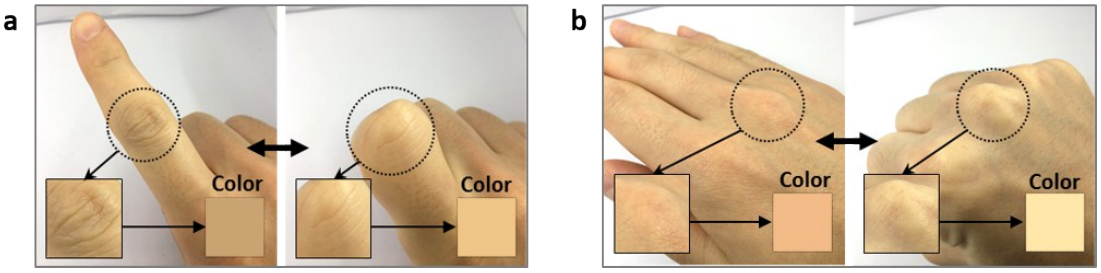

Figure S1. Photograph of (a) finger and (b) back-of-the-hand joints, showing changes in skin color with application of strain.

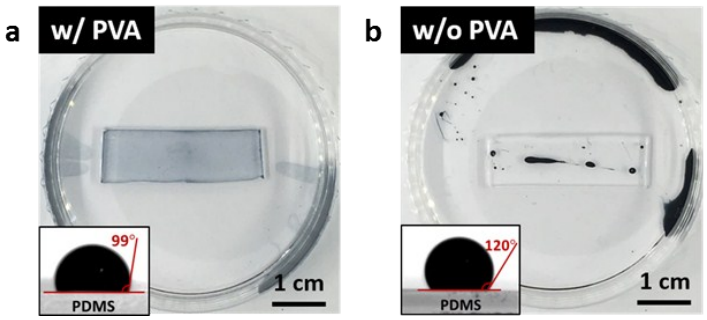

Figure S2. Photograph of spin-coated nanocomposite on PDMS substrate (a) with and (b) without PVA. The inset shows contact angles.

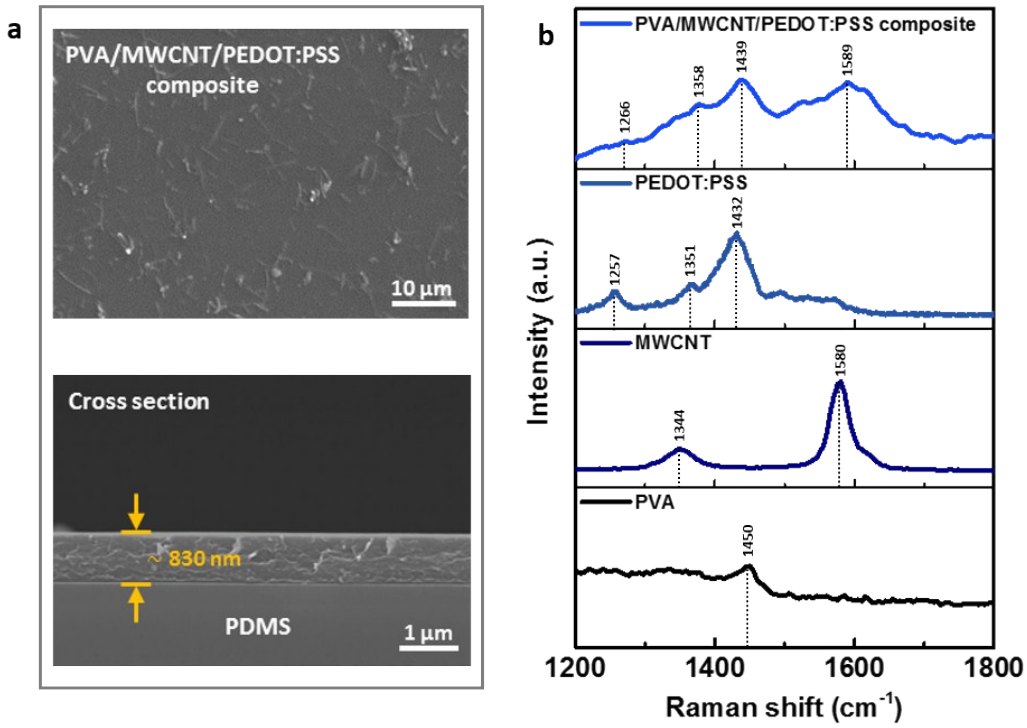

Figure S3. (a) Top and cross-sectional SEM images and (b) Raman spectra of PVA, MWCNT, PEDOT:PSS, and PVA/MWCNT/PEDOT:PSS composite.

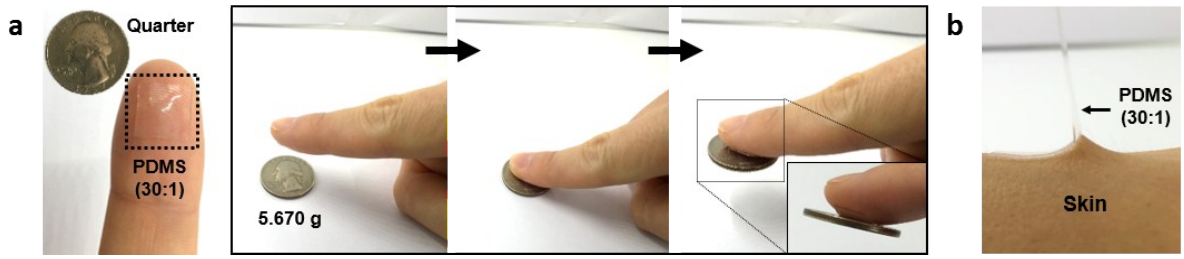

Figure S4. (a) The PDMS (30:1) conformally attached to the fingertip with a coin. (b) Photograph of the PDMS (30:1) adhesion to the skin of the hand.

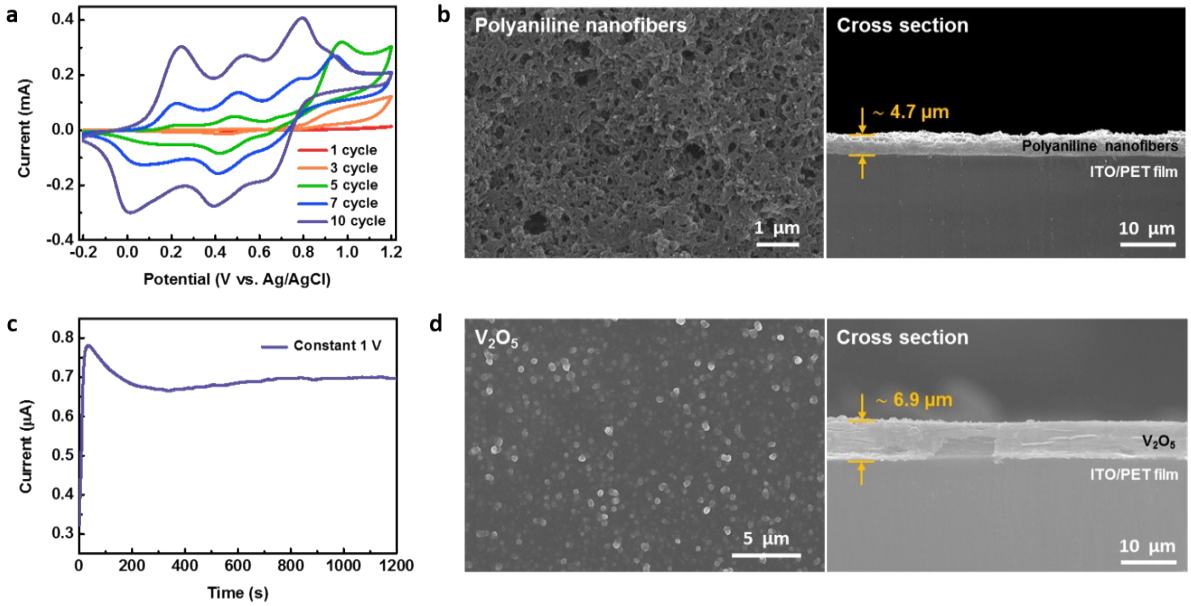

Figure S5. (a) CV curves of polyaniline nanofiber film with 10 deposition cycles at a constant scan rate of 50 mV s^{-1}. (b) Top and cross-sectional SEM images of polyaniline nanofibers. (c) Current–time response at a constant voltage of 1 V for 1200 s. (d) Top and cross-sectional SEM images of V_2O_5 films.

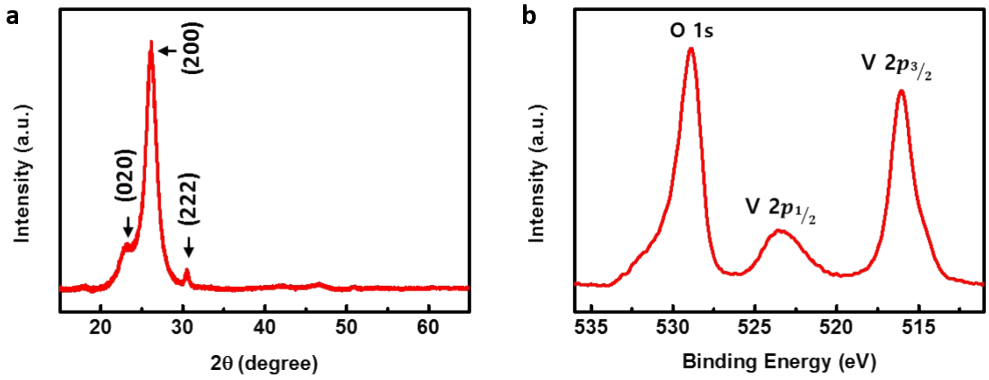

Figure S6. (a) X-ray diffraction (XRD) pattern of the polyaniline nanofiber film and (b) X-ray photoelectron spectroscopy (XPS) spectra of the V_2O_5 film.

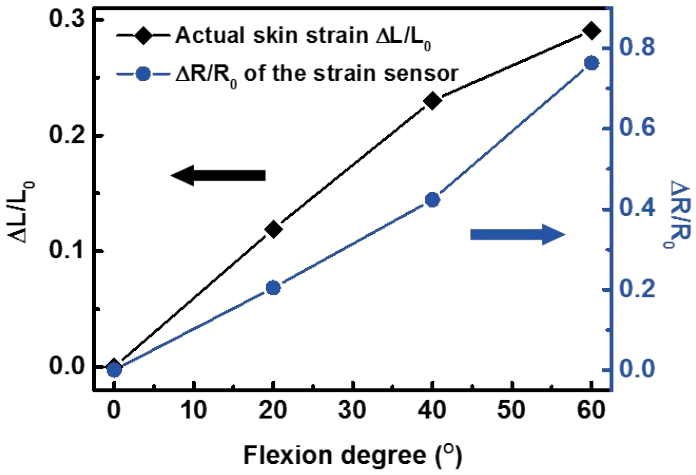

Figure S7. Measurement of the actual strain of the finger joint flexion movements with the degree of bending and the response of the strain sensor.

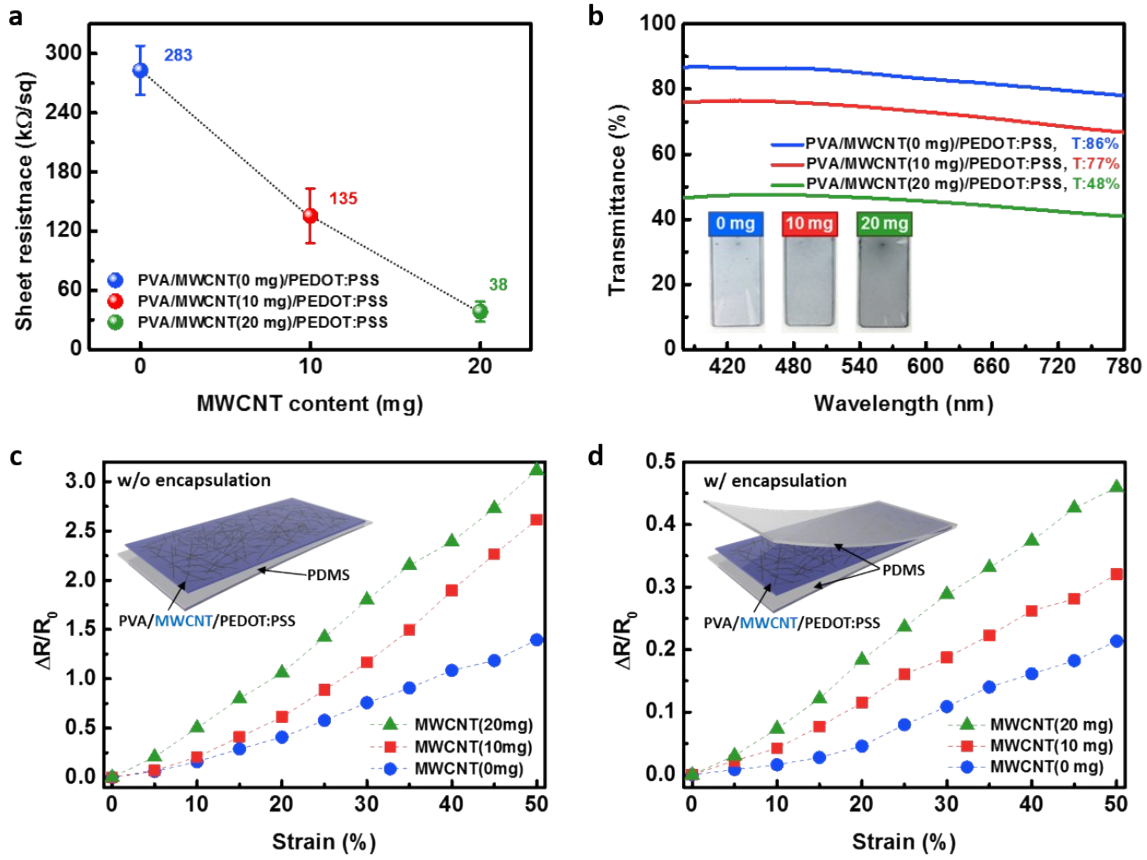

Figure S8. (a) Sheet resistance of the composite film as a function of MWCNT concentration. (b) Optical transmittance in the visible range from 380 to 780 nm for composite with MWCNT concentrations of 0, 10, and 20 mg. Relative change in resistance vs. strain of the PVA/MWCNT/PEDOT:PSS nanocomposite film at different MWCNT concentrations (c) without and (d) with encapsulation.

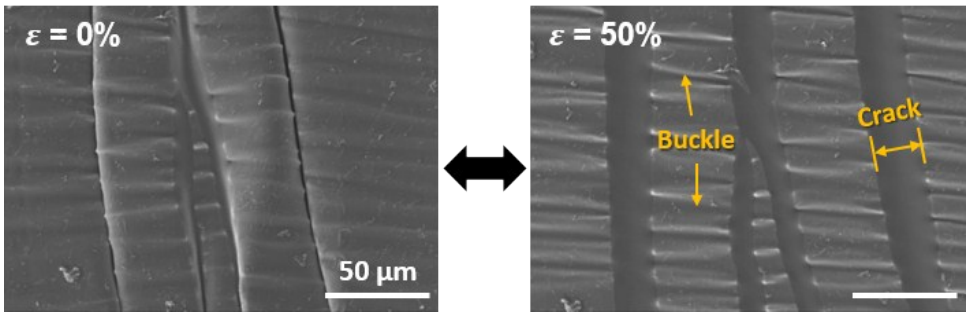

Figure S9. SEM images of surface cracks and buckles on the nanocomposite film at $\varepsilon = 0\%$ and $\varepsilon = 50\%$, respectively.

Poisson's ratio for the nanocomposite ($\nu_{nanocomposite}$) can be calculated by the rule of mixture; i.e., $\nu_{nanocomposite} = \nu_{PEDOT:PSS} f_{PEDOT:PSS} + \nu_{MWCNT} f_{MWCNT} + \nu_{PVA} f_{PVA}$, where $\nu_{PEDOT:PSS}$, $f_{PEDOT:PSS}$, ν_{MWCNT}, f_{MWCNT}, ν_{PVA}, and f_{PVA} represent the Poisson ratio for PEDOT:PSS (0.33), MWCNT (0.06), and PVA (0.42–0.48, average 0.45) and the volume fraction of PEDOT:PSS (0.966), MWCNT (0.001), and PVA (0.033), respectively. From these equations, we can estimate $\nu_{nanocomposite}$ as 0.34.[1-5] Poisson's ratio for PDMS (30:1) is 0.5.[6]

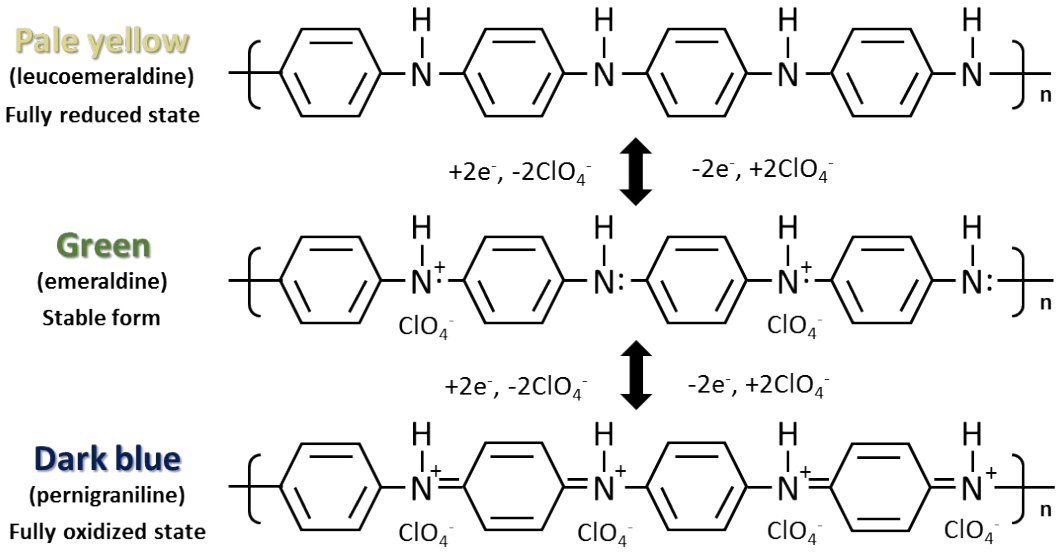

Figure S10. Chemical structures of different redox forms of polyaniline nanofibers.

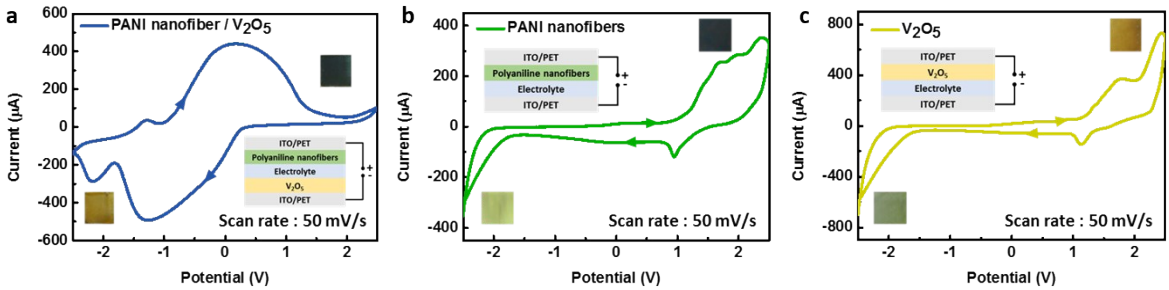

Figure S11. CV curves of (a) polyaniline nanofibers / V_2O_5, (b) polyaniline nanofibers, and (c) V_2O_5 films, at a scan rate of 50 mV s^{-1}.

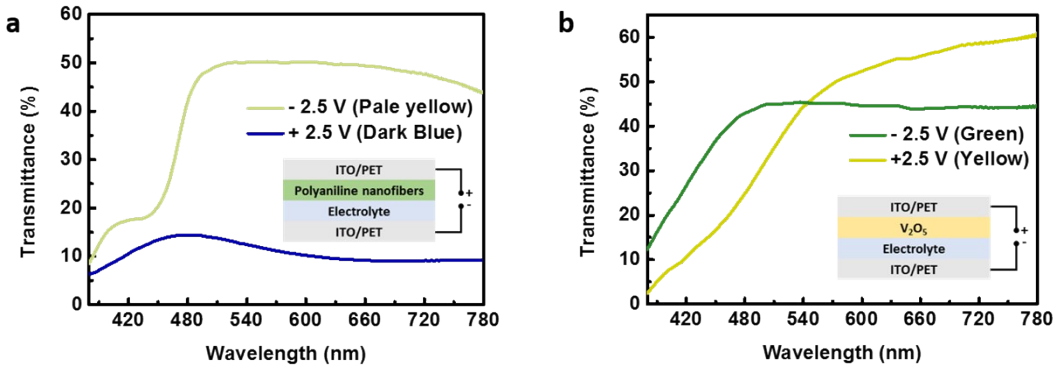

Figure S12. Transmittance spectra for the electrochromic device of (a) polyaniline nanofibers and (b) V_2O_5, measured at −2.5 V and +2.5 V.

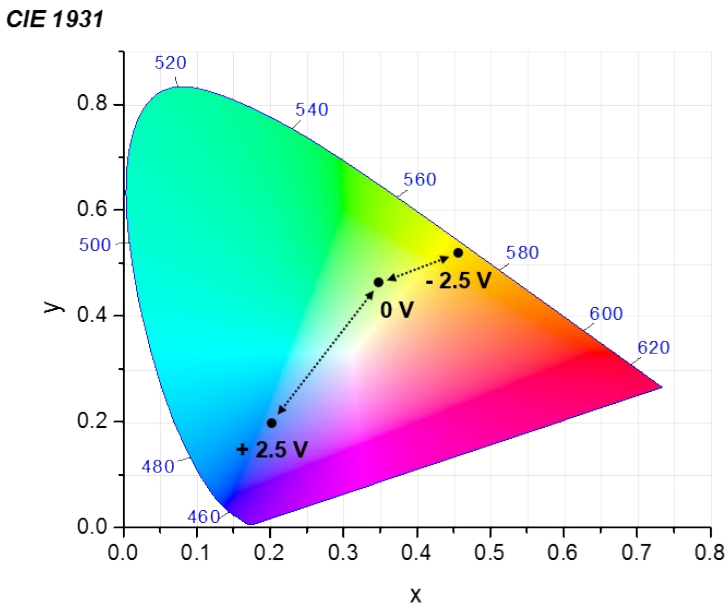

Figure S13. CIE 1931 Y_{xy} chromaticity diagram of ECD depending on different applied potentials.

The CIE chromaticity values (x, y) are (0.472, 0.517), (0.351, 0.455), and (0.202, 0.197) at -2.5 V, 0 V, and +2.5 V, respectively.

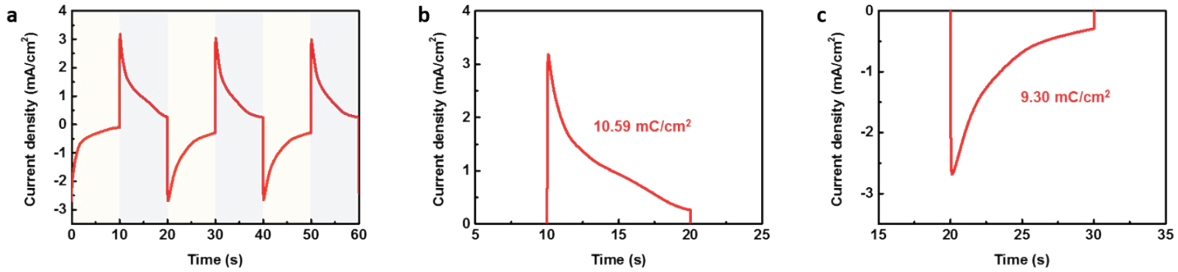

Figure S14. (a) Current change when switching between −2.5 V and +2.5 V. (b), (c) Enlargement of the charging and the discharging part, respectively.

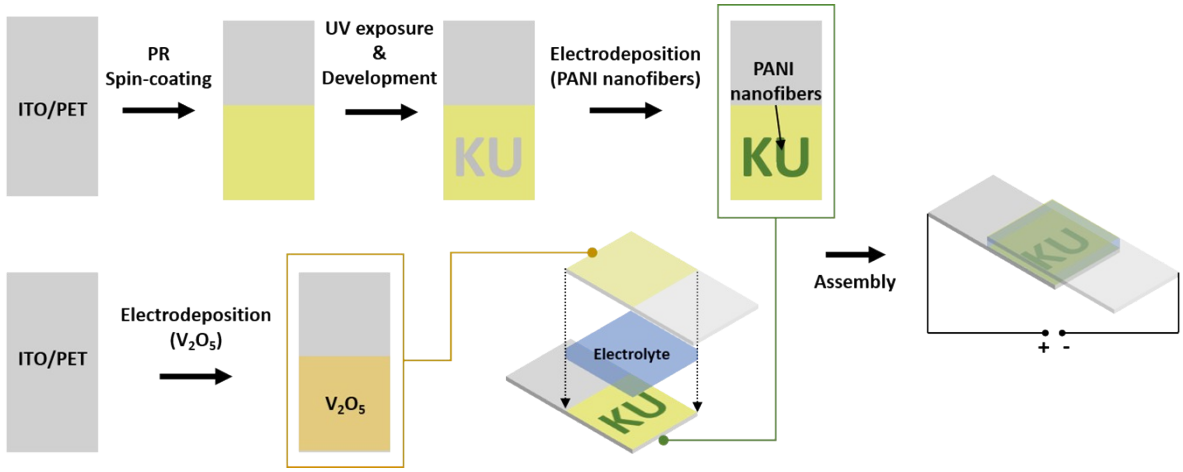

Figure S15. Schematic illustration showing the fabrication of the patterned electrochromic device for character display.

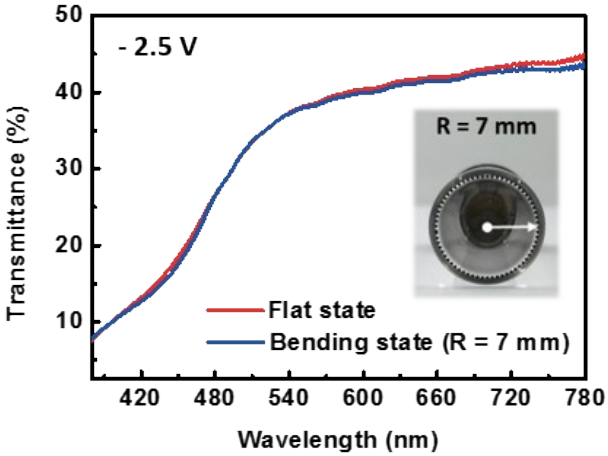

Figure S16. Transmittance spectra of the electrochromic device at −2.5 V under flat (red) and bent (blue) states.

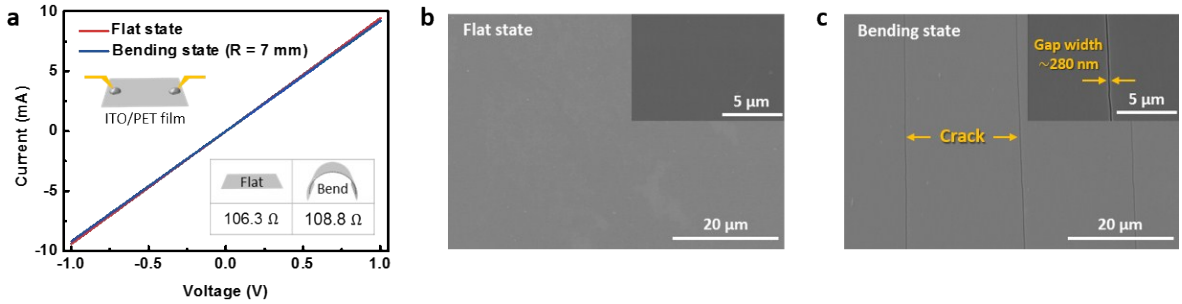

Figure S17. (a) I–V curves; and (b), (c) SEM images of the ITO/PET electrode in flat and bending states, respectively.

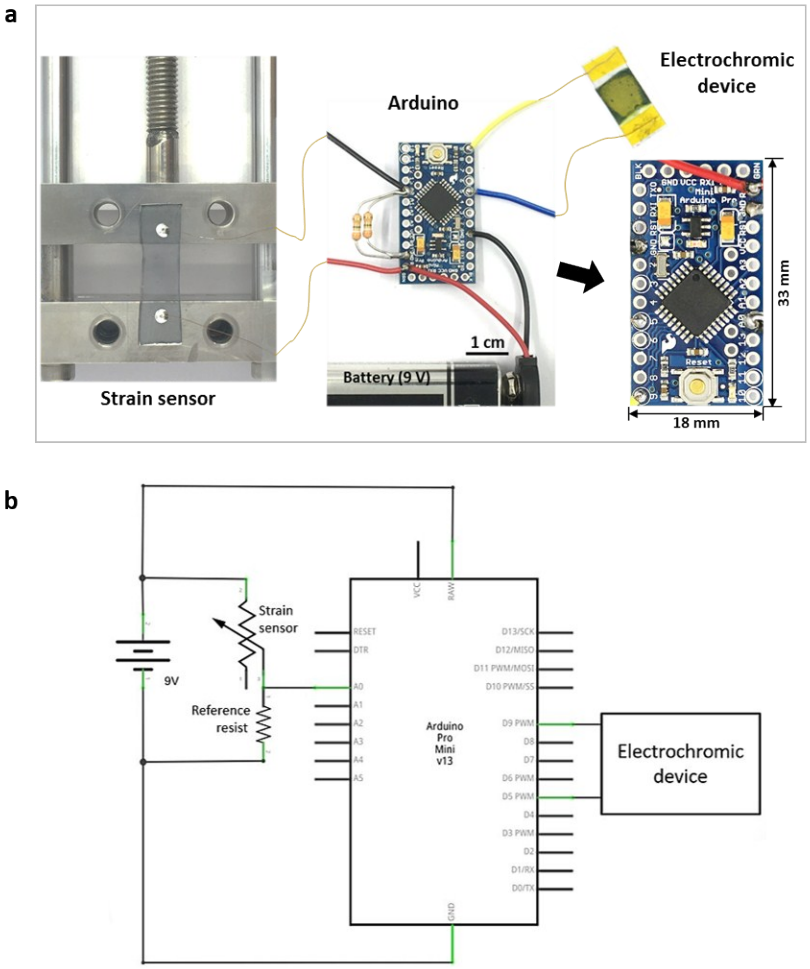

c

```
int inputVoltage=0;
int negativeVout=0;
int positiveVout=0;

void setup() {
Serial.begin(9600);
}

void loop() {

int inputVoltage=analogRead(A0);

if(inputVoltage>922)
{
int negativeVout=127;
analogWrite(9,negativeVout);
int positiveVout=0;
analogWrite(5,positiveVout);
}

else if(inputVoltage<=922 &&
inputVoltage>=917)
{

negativeVout=map(inputVoltage,921,869,127,
0);
 analogWrite(9,negativeVout);
 int positiveVout=0;
analogWrite(5,positiveVout);
}
else if(inputVoltage<=869 &&
inputVoltage>=817)
{

positiveVout=map(inputVoltage,869,817,0,127
);
 analogWrite(5,positiveVout);
 int negativeVout=0;
 analogWrite(9,negativeVout);
}
else if(inputVoltage<817)
{
int negativeVout=0;
analogWrite(9,negativeVout);
int positiveVout=127;
analogWrite(5,positiveVout);
}
delay(100);
 Serial.print("positiveVout : ");
 Serial.print(positiveVout);
 Serial.print(" and negativeVout : ");
 Serial.print(negativeVout);
 Serial.print("  -->intputVoltage : ");
 Serial.println(inputVoltage);


}
```

Figure S18. (a) Photograph and (b) circuit of the integrated system. (c) The source code for Arduino.

Arduino applies a bias voltage (V_{out}) across the ECD in accordance with the voltage (V_{in}) across the reference resistance (R_r), which is governed by the internal code. At 0% strain, V_{in} is 4.5 V because R_r is almost the same as the resistance of the strain sensor (R_s) at 0%. As the strain increases, V_{in} decreases linearly. When the strain varies from 0 to 30%, V_{out} changes from −2.5 V to +2.5 V.

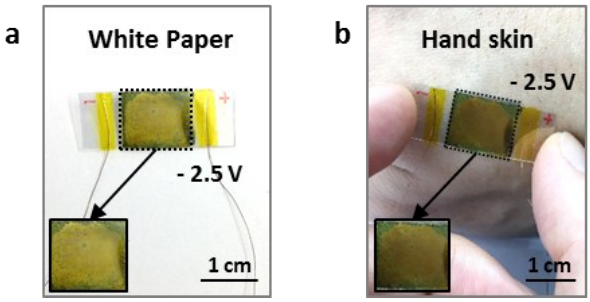

Figure S19. Optical images of electrochromic device on (a) white paper and (b) hand skin.

Table S1. Performance compared with data from previous studies on stretchable strain sensors.

Materials	Gauge Factor (GF)	Stretchability [%]	Transparency [%]	Durability Test [cycles]	Ref.
AgNP	2.05	20	Not shown	1000	7
Cracked Pt	2000	2	Not shown	5000	8
SWCNT	0.82	280	Not shown	10,000	9
Graphene	14	7.1	75–80	Not proven	10
Graphene woven fabrics (GWFs)	10^6	<10	Not shown	100	11
ZnO NW/polystyrene	116	50	16	>120	12
Carbon black(CB)+Toluene+PDMS composite	5.5	10	Not shown	30	13
AgNW+Elastomer composite	14	70	Not shown	1000	14
CNT+Polyurethane composite	69	400	Not shown	90	15
CNT+Chewing gum composite	25	530	Not shown	1000	16
SWCNT/PUD+PEDOT:PSS composite	62.7	100	63	1000	17
AgNW+PUD+PEDOT:PSS composite	12.4	100	75.3	1000	18
PVA+MWCNT+PEDOT:PSS composite	5.2	50	77	10,000	Our work

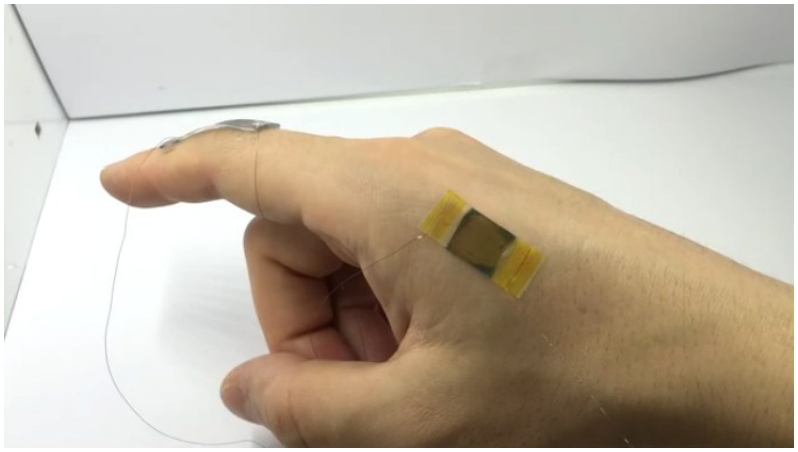

Supplementary Movie S1. Color change of ECD with finger bending.

References

1. J. H. Jung, M. Lee, J.-I. Hong, Y. Ding, C.-Y. Chen, L.-J. Chou and Z. L. Wang, *ACS Nano*, 2011, **5**, 10041-10046.
2. H. S. Kim, S. I. Hong and S. J. Kim, *J. Mater. Process. Technol.*, 2001, **112**, 109-113.
3. F. Greco, A. Zucca, S. Taccola, A. Menciassi, T. Fujie, H. Haniuda, S. Takeoka, P. Dario and V. Mattoli, *Soft Matter*, 2011, **7**, 10642-10650.
4. L. J. Hall, V. R. Coluci, D. S. Galvão, M. E. Kozlov, M. Zhang, S. O. Dantas and R. H. Baughman, *Science*, 2008, **320**, 504-507.
5. J. Fromageau, E. Brusseau, D. Vray, G. Gimenez and P. Delachartre, *IEEE Trans. Ultrason., Ferroelect., Freq. Control*, 2003, **50**, 1318-1324.
6. N. Juthani, C. Howell, H. Ledoux, I. Sotiri, S. Kelso, Y. Kovalenko, A. Tajik, T. L. Vu, J. J. Lin, A. Sutton and J. Aizenberg, *Sci. Rep.*, 2016, **6**, 26109.
7. J. Lee, S. Kim, J. Lee, D. Yang, B. C. Park, S. Ryu and I. Park, *Nanoscale*, 2014, **6**, 11932-11939.
8. D. Kang, P. V. Pikhitsa, Y. W. Choi, C. Lee, S. S. Shin, L. Piao, B. Park, K.-Y. Suh, T.-i. Kim and M. Choi, *Nature*, 2014, **516**, 222-226.
9. T. Yamada, Y. Hayamizu, Y. Yamamoto, Y. Yomogida, A. Izadi-Najafabadi, D. N. Futaba and K. Hata, *Nat. Nanotechnol.*, 2011, **6**, 296-301.
10. S.-H. Bae, Y. Lee, B. K. Sharma, H.-J. Lee, J.-H. Kim and J.-H. Ahn, *Carbon*, 2013, **51**, 236-242.
11. X. Li, R. Zhang, W. Yu, K. Wang, J. Wei, D. Wu, A. Cao, Z. Li, Y. Cheng, Q. Zheng, R. S. Ruoff and H. Zhu, *Sci. Rep.*, 2012, **2**, 870.
12. X. Xiao, L. Yuan, J. Zhong, T. Ding, Y. Liu, Z. Cai, Y. Rong, H. Han, J. Zhou and Z. L. Wang, *Adv. Mater.*, 2011, **23**, 5440-5444.
13. J.-H. Kong, N.-S. Jang, S.-H. Kim and J.-M. Kim, *Carbon*, 2014, **77**, 199-207.

14. M. Amjadi, A. Pichitpajongkit, S. Lee, S. Ryu and I. Park, *ACS Nano*, 2014, **8**, 5154-5163.

15. P. Slobodian, P. Riha, R. Benlikaya, P. Svoboda and D. Petras, *IEEE Sens. J.*, 2013, **13**, 4045-4048.

16. M. A. Darabi, A. Khosrozadeh, Q. Wang and M. Xing, *ACS Appl. Mater. Interfaces*, 2015, **7**, 26195-26205.

17. E. Roh, B.-U. Hwang, D. Kim, B.-Y. Kim and N.-E. Lee, *ACS Nano*, 2015, **9**, 6252-6261.

18. B.-U. Hwang, J.-H. Lee, T. Q. Trung, E. Roh, D.-I. Kim, S.-W. Kim and N.-E. Lee, *ACS Nano*, 2015, **9**, 8801-8810.